Journal of Statistical Physics, Vol. 90, Nos. 5/6, 1998

A High-Order Accurate Algorithm for Electrostatics of Overlapping Disks

Johan Helsing[1]

Received August 19, 1997; final November 14, 1997

A fast and accurate algorithm for the computation of effective electric and mathematically equivalent properties of composites with nonsmooth interfaces is reported. The algorithm is based on an integral equation reformulation of the electrostatic partial differential equation and a fast hierarchical technique for potential field evaluation. In a numerical example, 200 large and strongly inhomogeneous aggregates of randomly overlapping disks are solved with a relative error of 0.0005.

KEY WORDS: Continuum percolation; disordered media; integral equations; effective conductivity; overlapping cylinders; large-scale calculations; fiber-reinforced materials.

I. INTRODUCTION

Random aggregates of overlapping objects are frequently studied geometries in the physics of disordered media: Objects with physical properties described by certain moduli are placed, at random, in a matrix with different moduli.

Much work for random aggregates concerns effective properties. Of particular interest, and difficulty, is to predict effective properties of highly inhomogeneous aggregates close to the continuum percolation threshold,[1, 2] that is, close to the area fraction for which the randomly placed objects start to form a connected path through the material. Popular numerical methods for this problem are often based on statistical ideas and include biased diffusion,[3] Monte Carlo or random walk simulations,[4, 5] "blind-ant"

[1] Department of Solid Mechanics, Royal Institute of Technology, SE-100 44 Stockholm, Sweden.

0022-4715/98/0300-1461$15.00/0

algorithms,[6] resistor network approximations,[7,8] and series expansion incorporating structural parameters.[9–11] Most of these methods converge as $1/\sqrt{N}$, where N is the computational work. A typical relative error for the effective moduli of strongly inhomogeneous large aggregates is on the order of 0.05. The justification for using low-order accurate methods seems to be a notion that high-order accurate methods are impossible to apply. The most reliable estimates for large random systems, until now, are perhaps experimental measurements on steel and molybdenum sheets[12] and thin aluminum films[13] with drilled holes.

This paper demonstrates that the accurate numerical calculation of effective properties of strongly inhomogeneous large random aggregates of overlapping objects is not only possible, but also simple to perform on a regular workstation. We specialize to overlapping disks and compute the effective conductivity for unit cells at two hundred different area fractions and with a relative error of 0.0005. At percolation the unit cells contain around 3,500 disks. The key ingredients in our algorithm are: (1) A new integral equation formulation for the electrostatic PDE on a doubly periodic domain. (2) The Fast Multipole Method for potential field evaluations.[14–16] (3) A recent algorithm for the evaluation of layer potentials close to their sources.[17]

II. INTEGRAL EQUATIONS AND EFFECTIVE PROPERTIES

This section reviews integral equation reformulations of the electrostatic PDE for two-dimensional two-component composite materials. The material's geometry is given in a unit cell, taken to be the square $D_0 = (-1/2, 1/2] \times (-1/2, 1/2]$, and periodically repeated as to tile the entire plane. The area fractions and the conductivities of the components are p_1, p_2, σ_1, and σ_2. If one component forms at least one infinitely large connected region while the other component forms finite regions the composite is called a suspension of inclusions. The interfaces between the components in the unit cell are called Γ_{unit}. The interfaces Γ_{unit} and their periodic images are called Γ. The interfaces Γ and the parts of the unit cell boundary that are covered with component two and their periodic images are called Γ_{ext}.

An average electric field $\mathbf{e}$ of unit strength is applied to the composite. The potential $U_{\mathbf{r}}$ at position $\mathbf{r}$ in the composite can then be represented on the form

$$U_{\mathbf{r}} = \mathbf{e} \cdot \mathbf{r} + \frac{1}{2\pi} \int_{\Gamma} \log |\mathbf{r} - \mathbf{r}_t| \, \rho_t \, \mathrm{d}t \tag{1}$$

where ρ is an unknown density and $\mathbf{r}_t$ and ρ_t denote position and density at arclength t. The density ρ can be solved for from the integral equation

$$2\mathbf{e}\cdot\mathbf{n}_s=\frac{(\sigma_2+\sigma_1)}{(\sigma_2-\sigma_1)}\rho_s+\frac{1}{\pi}\int_\Gamma \frac{\mathbf{n}_s\cdot(\mathbf{r}_t-\mathbf{r}_s)}{|\mathbf{r}_t-\mathbf{r}_s|^2}\rho_t\,dt \tag{2}$$

where $\mathbf{n}_s$ is the unit normal at arclength s pointing into component one. Equation (2) follows from insertion of Eq. (1) into the electrostatic PDE. If the composite is a suspension where no inclusion overlaps the unit cell boundary, and if component one denotes the matrix, the effective conductivity σ_{eff} in the direction $\mathbf{e}$ can be written

$$\sigma_{\text{eff}}=\sigma_1+\sigma_1\int_{\Gamma_{\text{unit}}}\mathbf{e}\cdot\mathbf{r}_s\rho_s\,ds \tag{3}$$

Equation (2) is the choice of Greengard and Moura[18] in their pioneering work on the electrostatics of large suspensions, and of Cheng and Greengard[19] in their work on random suspensions of non-overlapping disks.

If the composite is a suspension where inclusions do overlap the unit cell boundary, the effective conductivity can still be computed from Eq. (3) after a modification of the shape of the unit cell. If the composite is not a suspension Eq. (3) does not apply without more extensive modifications. Another possibility is to use the formula

$$\sigma_{\text{eff}}=\int_{\mathbf{r}=(0.5,\,-0.5)}^{\mathbf{r}=(0.5,\,0.5)}\sigma_{\mathbf{r}}\frac{\partial U_{\mathbf{r}}}{\partial\mathbf{n}}\,dt \tag{4}$$

where the integral goes along the unit cell boundary and where a shorthand notation for the directional derivative is used.

There are many ways to represent the potential $U_{\mathbf{r}}$ in the composite. Equation (1), the single layer representation, is just a convenient choice. Another integral formulation is based on the representation

$$U_{\mathbf{r}}=-\frac{1}{2\pi}\int_\Gamma\frac{\mathbf{n}_t\cdot(\mathbf{r}_t-\mathbf{r})}{|\mathbf{r}_t-\mathbf{r}|^2}U_t\,dt-\frac{1}{2\pi}\int_\Gamma\log|\mathbf{r}-\mathbf{r}_t|\frac{\partial U_t}{\partial\mathbf{n}}\,dt \tag{5}$$

In terms of a scaled potential $u_{\mathbf{r}}$ defined by

$$u_{\mathbf{r}}=\frac{(\sigma_2-\sigma_1)}{\sigma_1}U_{\mathbf{r}} \tag{6}$$

and with the use of Green's second identity, an integral equation can be derived

$$2\mathbf{e}\cdot\mathbf{r}_s=\frac{(\sigma_2+\sigma_1)}{(\sigma_2-\sigma_1)}u_s-\frac{1}{\pi}\int_\Gamma \frac{\mathbf{n}_t\cdot(\mathbf{r}_t-\mathbf{r}_s)}{|\mathbf{r}_t-\mathbf{r}_s|^2}u_t\,\mathrm{d}t \tag{7}$$

The effective conductivity in the direction $\mathbf{e}$ can be computed from u via

$$\sigma_{\text{eff}}=\sigma_1+\sigma_1\int_{\Gamma_{\text{unit}}}\mathbf{e}\cdot\mathbf{n}_s u_s\,\mathrm{d}s \tag{8}$$

The integral kernels in Eq. (2) and Eq. (7) are each other's adjoints. One could therefore expect that the amount of work needed to solve the two equations with a given error tolerance should be similar. A closer inspection reveals a difference between the equations: the left hand side in Eq. (7) is a smoother quantity than the left hand side in Eq. (2). Does this mean that Eq. (7) is easier to solve than Eq. (2)? As we shall see in the next section, the answer to this question is often "yes." An difficulty with Eq. (7) is that it calls for integration involving a non-periodic and unbounded function, $u_{\mathbf{r}}$, over an infinite domain.

We now propose a reformulation of Eq. (7) that is a simplification from a numerical viewpoint: First the potential $u_{\mathbf{r}}$ is split up into a linearly growing and into a periodic and bounded part

$$u_{\mathbf{r}}=\frac{(\sigma_2-\sigma_1)}{\sigma_1}\mathbf{e}\cdot\mathbf{r}+w_{\mathbf{r}} \tag{9}$$

Then Eq. (7) is rewritten

$$\begin{aligned}-\frac{(\sigma_2-\sigma_1)}{\sigma_1}\mathbf{e}\cdot\mathbf{r}_s+\frac{(\sigma_2-\sigma_1)}{\sigma_1}\frac{1}{\pi}\int_{\Gamma_{\text{ext}}}\frac{\mathbf{n}_t\cdot(\mathbf{r}_t-\mathbf{r}_s)}{|\mathbf{r}_t-\mathbf{r}_s|^2}\mathbf{e}\cdot\mathbf{r}_t^*\,\mathrm{d}t\\ =\frac{(\sigma_2+\sigma_1)}{(\sigma_2-\sigma_1)}w_s-\frac{1}{\pi}\int_\Gamma\frac{\mathbf{n}_t\cdot(\mathbf{r}_t-\mathbf{r}_s)}{|\mathbf{r}_t-\mathbf{r}_s|^2}w_t\,\mathrm{d}t\end{aligned} \tag{10}$$

where $\mathbf{r}^*$ is the position $\mathbf{r}$ translated with a lattice vector back into the unit cell. Equation (8) becomes

$$\sigma_{\text{eff}}=p_1\sigma_1+p_2\sigma_2+\sigma_1\int_{\Gamma_{\text{unit}}}\mathbf{e}\cdot\mathbf{n}_s w_s\,\mathrm{d}s \tag{11}$$

In Eq. (10) the integral on the left hand side includes parts of the unit cell boundary. This integral is simple, since it only involves known geometric quantities.

Yet another choice for the potential is the layer representation

$$U(\mathbf{r}) = \mathbf{e}\cdot\mathbf{r} - \frac{1}{2\pi}\int_\Gamma \frac{\mathbf{n}_{\perp t}\cdot(\mathbf{r}_t-\mathbf{r})}{|\mathbf{r}_t-\mathbf{r}|^2}\mu_t\,\mathrm{d}t \tag{12}$$

where $\mathbf{n}_{\perp t}$ is the unit tangential vector at t, pointing in positive direction. The electrostatic PDE leads to the integral equation

$$2\mathbf{e}_\perp\cdot\mathbf{r}_s = \frac{(\sigma_2+\sigma_1)}{(\sigma_2-\sigma_1)}\mu_s + \frac{1}{\pi}\int_\Gamma \frac{\mathbf{n}_t\cdot(\mathbf{r}_t-\mathbf{r}_s)}{|\mathbf{r}_t-\mathbf{r}_s|^2}\mu_t\,\mathrm{d}t \tag{13}$$

where $\mathbf{e}_\perp$ is the vector $\mathbf{e}$ rotated 90 degrees counter-clockwise. The effective conductivity in the direction $\mathbf{e}$ is

$$\sigma_{\text{eff}} = \sigma_1 + \sigma_1\int_{\Gamma_{\text{unit}}} \mathbf{e}_\perp\cdot\mathbf{n}_s\mu_s\,\mathrm{d}s \tag{14}$$

While Eq. (12) may be simpler to evaluate than Eq. (5), the integral Eq. (13) is rather similar to the integral Eq. (7) and it will not be discussed further in this paper.

III. NUMERICAL COMPARISON OF INTEGRAL EQUATIONS

In this section we compare the performance of Eqs. (2) and (3), Eqs. (2) and (4) and Eqs. (10) and (11) for various composites with different kinds of interfaces. In all examples we choose $\sigma_1 = 1$ and $\sigma_2 = 1000$. For the numerical solution of the integral equation we use a recent Nyström algorithm[17] which relies on 16-point Gauss–Legendre quadrature with aposteriori refinement, solution of systems of linear equations with the GMRES[20] iterative solver, an adaptive method for evaluation of layer potentials close to their sources, and Fast Multipole Method[14 16] acceleration of matrix-vector multiplication. Initially, we place eight Gaussian segments per disk. For each stage of adaptive refinement we increase the number of segments with about 25%. The "tolerance" is the value of the residual below which GMRES iteration is terminated. This value is chosen experimentally as to give the highest achievable accuracy with the fewest number of iterations for each stage.

A. Suspensions with Smooth Interfaces

We first look at a suspension with smooth interfaces: the random suspension of equisized disks shown in Fig. 1 where $p_2 = 0.6$. Table I shows

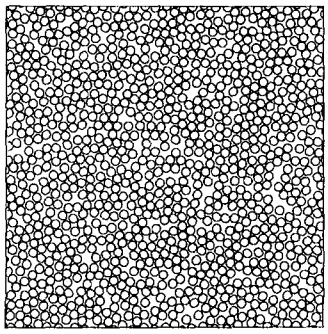

Fig. 1. A unit cell with a "random" suspension of 1024 disks at area fraction $p_2 = 0.6$.

that for very high resolution, Eqs. (10) and (11) and Eqs. (2) and (3) perform similarly. For lower resolution Eqs. (10) and (11) gives better accuracy than Eqs. (2) and (3).

B. Suspensions with Nonsmooth Interfaces

We next turn to a suspension with nonsmooth interfaces: the arrangement of 902 overlapping disks shown in Fig. 2. The disks have radius $R = 0.02$. In the left arrangement the disks are placed at random with the constraint that no disks overlap the unit cell boundary. In this way we make sure that the material is a suspension and that Eq. (3) applies. The right arrangement is the same as the left arrangement, the difference being that all disks are translated so that there is a considerable number of disks

Table I. Effective Conductivity in the *x*-Direction for the "Random" Suspension of 1024 Disks in Fig. 1[a]

	Stage 1	Stage 2	Stage 3	Stage 4
σ_{eff}, Eq. (3)	5	15.14	5.14079	5.14078902
σ_{eff}, Eq. (11)	5.14	15.1408	5.140789	5.14078902
iterations, Eq. (2)	39	27	56	72
iterations, Eq. (10)	51	53	67	82
points, Eq. (2)	131,072	180,224	229,376	278,528
points, Eq. (10)	131,936	181,088	229,696	277,136
tolerance, Eq. (2)	10^{-2}	10^{-2}	10^{-4}	10^{-7}
tolerance, Eq. (10)	10^{-6}	10^{-7}	10^{-9}	10^{-11}

[a] The infinite medium has conductivity $\sigma_1 = 1$ and the disks have conductivity $\sigma_2 = 1000$. The value in the limit of an infinitely large unit cell should be 5.114 ± 0.060.[19]

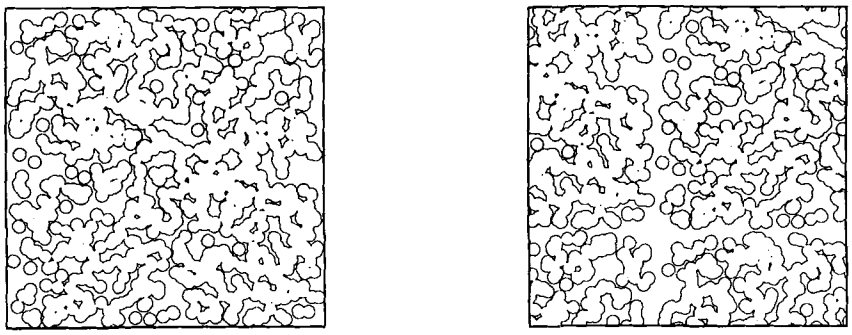

Fig. 2. The left image depicts a unit cell consisting of 902 overlapping disks of radius $R = 0.02$. The area fraction is $p_2 \approx 0.65506$. The disk are placed at random with the constraint that no disk must overlap the unit cell boundary. The right image depicts the same material, but the origin is translated so that many disks now overlap the unit cell boundaries.

that overlap the unit cell boundary. Table II shows that Eqs. (10) and (11) give better accuracy than Eqs. (2) and (3), which in turn give better accuracy than Eqs. (2) and (4), for all stages of resolution. Furthermore, for Eqs. (10) and (11) no accuracy is lost when the inclusions are allowed to overlap the unit cell boundary.

Table II. Effective Conductivity in the *x*-Direction for the Aggregate of 902 Disks in Fig. 2[a]

	Stage 1	Stage 2	Stage 3	Stage 6	Stage 9
σ_{eff}, left image, Eq. (3)	15.10	15.10	15.10	15.10	15.10
σ_{eff}, right image, Eq. (4)	15	15.1	15.1	15.1	15.10
σ_{eff}, both images, Eq. (11)	15.098	15.0976	15.0976	15.09762	15.09762
iterations, left image, Eq. (2)	78	80	83	94	107
iterations, left image, Eq. (10)	95	113	113	129	129
iterations, right image, Eq. (10)	91	91	91	125	124
points, left image, Eq. (2)	55,264	69,072	77,856	100,480	122,320
points, left image, Eq. (10)	55,264	69,072	77,840	102,240	124,848
points, right image, Eq. (10)	55,648	69,522	82,992	122,368	161,600
tolerance, Eq. (2)	10^{-4}	10^{-4}	10^{-4}	10^{-4}	10^{-4}
tolerance, Eq. (10)	10^{-6}	10^{-7}	10^{-7}	10^{-8}	10^{-8}

[a] The infinite medium has conductivity $\sigma_1 = 1$ and the disks have conductivity $\sigma_2 = 1000$.

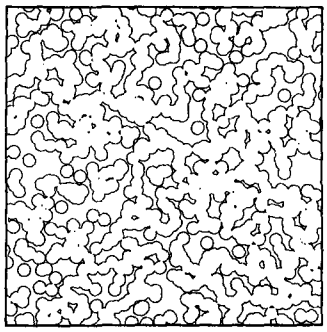

Fig. 3. A unit cell consisting of 902 overlapping disks of radius $R = 0.02$. The area fraction, $p_2 \approx 0.67528$, is close to the percolation threshold.

C. General Composites with Nonsmooth Interfaces

The arrangement in Fig. 3 has 902 randomly overlapping disks in the unit cell. The interfaces are nonsmooth and the unit cell boundary is covered with both types of components. The disks radius is $R = 0.02$ and the area fraction is $p_2 \approx 0.67528$—close to the percolation threshold. In this particular realization there is no percolation of disks in the x-direction. Table III shows that Eqs. (10) and (11) give roughly 100 times better accuracy than Eqs. (2) and (4), for a given amount of work.

Figure 4 shows an arrangement of 1763 randomly overlapping disks with radius $R = 0.01414$. The area fraction is $p_2 \approx 0.67530$. In this realization there is percolation of disks in the x-direction. Table IV shows that Eqs. (10) and (11) again give roughly 100 times better accuracy than Eqs. (2) and (4), for a given amount of work.

Table III. Effective Conductivity in the x-Direction for the Aggregate of 902 Disks in Fig. 3[a]

	Stage 1	Stage 2	Stage 3	Stage 6	Stage 9
σ_{eff}, Eq. (4)	48	48	48.3	48.3	48.3
σ_{eff}, Eq. (11)	48.32	48.322	48.322	48.3222	48.3222
iterations, Eq. (10)	101	120	120	135	135
points, Eq. (2)	57,744	72,176	82,032	105,728	128,592
points, Eq. (10)	58,096	72,608	83,856	115,856	146,560
tolerance, Eq. (10)	10^{-5}	10^{-6}	10^{-6}	10^{-7}	10^{-7}

[a] The infinite medium has conductivity $\sigma_1 = 1$. The disks have conductivity $\sigma_2 = 1000$.

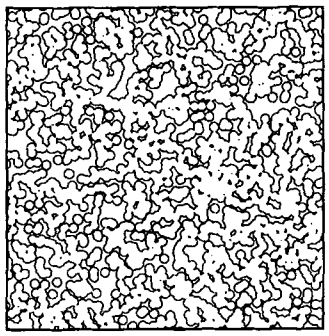

Fig. 4. A unit cell consisting of 1763 overlapping disks of radius $R = 0.01414$. The area fraction, $p_2 \approx 0.67530$, is close to the percolation threshold.

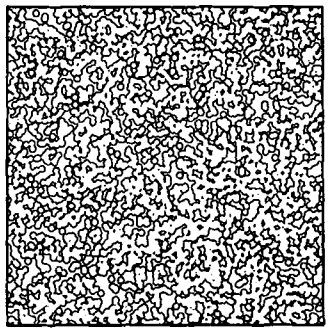

Fig. 5. A unit cell consisting of 3502 overlapping disks of radius $R = 0.01$. The area fraction, $p_2 \approx 0.67519$, is close to the percolation threshold.

Table IV. Effective Conductivity in the *x*-Direction for the Aggregate of 1763 Disks in Fig. 4[a]

	Stage 1	Stage 2	Stage 3	Stage 4
σ_{eff}, Eq. (4)	71	71	71	71.7
σ_{eff}, Eq. (11)	71.7	71.71	71.715	71.715
iterations, Eq. (10)	95	124	149	149
points, Eq. (2)	116,144	145,168	164,464	180,752
points, Eq. (10)	116,624	145,776	170,448	194,384
tolerance, Eq. (10)	10^{-5}	10^{-6}	10^{-7}	10^{-7}

[a] The infinite medium has conductivity $\sigma_1 = 1$ and the disks have conductivity $\sigma_2 = 1000$.

Table V. Effective Conductivity in the x-Direction for the Aggregate of 3502 Disks in Fig. 4[a]

	Stage 1	Stage 2
σ_{eff}, Eq. (11)	43.7 (43.696)	43.69 (43.6936)
iterations, Eq. (10)	88	155
points, Eq. (10)	236,144	295,168
tolerance, Eq. (10)	10^{-4}	10^{-6}

[a] The infinite medium has conductivity $\sigma_1 = 1$ and the disks have conductivity $\sigma_2 = 1000$. The numbers within perethesis denote the converged solutions at the two stages.

In the arrangement of 3502 randomly overlapping disks in Fig. 5 the disks radius is $R = 0.01$ and the area fraction is $p_2 \approx 0.67519$. In this realization there is no percolation of disks in the x-direction. The effective conductivity, presented in Table V, is even lower than that of the composite in Fig. 3.

Tables III, IV, and V demonstrate that for unit cells with several thousand randomly placed disks, close to the percolation threshold, and for a degree of inhomogeneity around a thousand, details in the microstructure do have influence on the effective conductivity. Tables III–V also tell us that for a relative error of 0.0005, and with Eqs. (10) and (11), it is sufficient to use only one stage of refinement and to stop the GMRES iterations when the residual is less than 10^{-5}.

IV. BULK CALCULATIONS

The previous section shows that Eqs. (10) and (11) can give effective properties for aggregates of overlapping disks with $R = 0.01$ and $\sigma_2/\sigma_1 = 1000$ with a relative accuracy of 0.0005 at a modest computational cost. In a final example we produce numerical results computed with Eqs. (10) and (11) to that same accuracy for 200 different unit cells sampling the entire range of area fractions $p_2 = 0.00$ to $p_2 = 1.00$. The results are shown in Fig. 6. The curve is rather smooth to the eye-indicating that the system can be considered "quite large" for the chosen degree of inhomogeneity. The computations took approximately 200 CPU hours on a SUN Ultra 1 workstation. The chosen problem size is perhaps close to what can be treated at present on a regular workstation without swapping. The bulk of the memory is used to store search directions in the Krylov space for the GMRES solver.

It is of interest to compare our computed effective properties to well-studied theoretical predictions such as bounds and effective medium

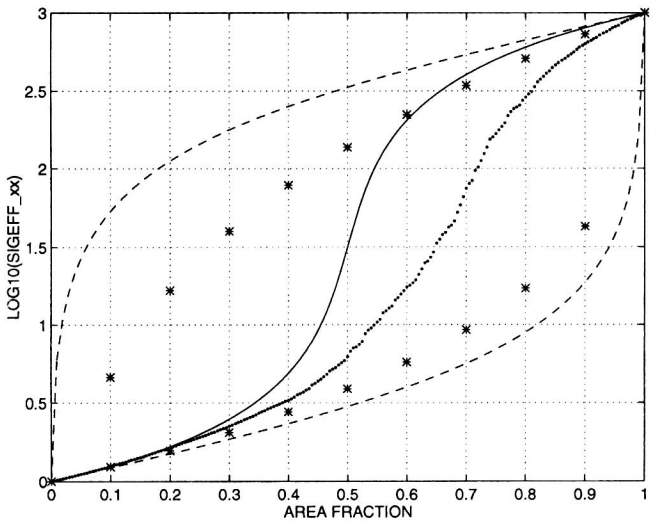

Fig. 6. The effective conductivity of random aggregates of overlapping disks in a unit cell at various area fractions along with bounds and a crude estimate. Points denote the computations in this paper, the dashed lines are the Hashin Shtrikman bounds,[21] the stars are a fourth order bound,[10,11] and the solid line is an effective medium approximation.[22] The disk radius is $R = 0.01$ and the conductivity of the matrix and of the disks are $\sigma_1 = 1$ and $\sigma_2 = 1000$.

approximations. Apart from being of theoretical interest, bounds and crude approximations give rapid answers in difficult situations when only partial geometric information about a composite is available or when the geometry is too complicated to be discretized. For these type of estimates to be quantitatively useful, however, the degree of inhomogeneity must not be too large. Figure 6 also shows the second order accurate Hashin–Shtrikman bounds,[21] a pair of fourth order accurate bounds derived by Milton[10] which incorporate structural data computed by Torquato and Beasley,[11] and the Bruggeman effective medium approximation[22] for disks. As we can see, the bounds are quite conservative and the effective medium approximation is acceptable only for low area fractions where the geometry resembles a dilute suspension of disks. Note that the vertical axis has a logarithmic scale.

V. DISCUSSION

The algorithm presented in this paper should be a powerful tool for the numerical investigation of conductivity behavior for continuum percolation in two dimensions. The geometry can be arbitrary. We chose disks in our examples because it is a standard choice.

The reader may wonder what the computational cost would be if the code was extended to three dimensions. Here follow some thoughts on that topic: The bulk of the computational work in the present two-dimensional algorithm is spent in the fast multipole routine inside the GMRES solver. We use the scheme of Greengard and Rokhlin.[15] Assuming N uniformly spaced discretization points in the unit cell and using seven digit accuray, the number of operations per iteration is between $200N$ and $300N$. The latest version of the fast multipole method for the Laplace equation in three dimensions[23] require approximately $2000N$ operations per iteration. The complexity of the fast multipole method in two and three dimensions is similar, while the actual work per GMRES iteration, given a number of points and a prescribed accuracy, could be ten times larger in three dimensions than in two dimensions.

While it is easy to find three dimensional analouges to the two dimensional integral equations used above, discretizing interfaces in two and three dimensions are programming tasks of different magnitude. In order to make the three dimensional code efficient one also needs to extend our method for evaluation of layer potentials close to their sources[17] to three dimensions. The difficulty in these tasks are issues of parameterization and interpolation.

The computer code used in this paper is available from the author upon request.

ACKNOWLEDGMENTS

I thank Leslie Greengard, Robert Kohn, and Ohad Levy for many useful discussions. This work was supported by NFR, TFR, and The Knut and Alice Wallenberg Foundation under TFR contract 96-977.

REFERENCES

1. B. I. Halperin, S. Feng, and P. N. Sen, Differences between lattice and continuum percolation transport exponents, *Phys. Rev. Lett.* **54**:2391 (1985).
2. J. P. Clerc, G. Giraud, J. M. Laugier, and J. M. Luck, The electrical conductivity of binary disordered systems, percolation clusters, fractals and related models, *Advances in Physics* **39**:191 (1990).
3. L. M. Schwartz, J. R. Banavar, and B. I. Halperin, Biased-diffusion calculations of electrical transport in inhomogeneous continuum systems, *Phys. Rev. B* **40**:9155 (1989).
4. J. Tobochnik, D. Laing, and G. Wilson, Random-walk calculation of conductivity in continuum percolation, *Phys. Rev. A* **41**:3052 (1990).
5. M. M. Tomadakis and S. V. Sotirchos, Transport through random arrays of conductive cylinders dispersed in a conductive matrix, *J. Chem. Phys.* **104**:6893 (1996).
6. E. J. Garboczi, M. F. Thorpe, M. S. DeVries, and A. R. Day, Universal conductivity curve for a plane containing random holes, *Phys. Rev. A* **43**:6473 (1991).

7. T. Elam, A. R. Kerstein, and J. J. Rehr, Critical properties of the void percolation problem for spheres, *Phys. Rev. Lett.* **52**:1516 (1984).
8. B. Berkowitz and R. Knight, Continuum percolation conductivity exponents in restricted domains, *J. Stat. Phys.* **80**:1415 (1995).
9. G. W. Milton, Bounds on the electromagnetic, elastic, and other properties of two-component composites, *Phys. Rev. Lett.* **46**:542 (1981).
10. G. W. Milton, Bounds on the elastic and transport properties of two-component composites, *J. Mech. Phys. Solids* **30**:177 (1982).
11. S. Torquato and J. D. Beasley, Bounds on the effective thermal conductivity of dispersions of fully penetrable cylinders, *Int. J. Engng. Sci.* **24**:415 (1986).
12. C. J. Lobb and M. G. Forrester, Measurement of nonuniversal critical behavior in a two-dimensional continuum percolating system, *Phys. Rev. B* **35**:1899 (1990).
13. K. H. Han, Z. S. Lim, and S. I. Lee, Experimental study of the conductivity exponent in a two-dimensional Swiss cheese percolating network, *Physica B* **167**:185 (1990).
14. V. Rokhlin, Rapid solution of integral equations of classical potential theory, *J. Comput. Phys.* **60**:187–207 (1985).
15. L. Greengard and V. Rokhlin, A fast algorithm for particle simulations, *J. Comput. Phys.* **73**:325 (1987).
16. J. Carrier, L. Greengard and V. Rokhlin, A fast adaptive multipole algorithm for particle simulations, *SIAM J. Sci. and Stat. Comput.* **9**:669–686 (1988).
17. J. Helsing, Thin bridges in isotropic electrostatics, *J. Comp. Phys.* **127**:142 (1996).
18. L. Greengard and M. Moura, On the numerical evaluation of electrostatic fields in composite materials, *Acta Numerica 1994* (Cambridge University Press, Cambridge, 1994), pp. 379–410.
19. H. Cheng and L. Greengard, On the numerical evaluation of electrostatic fields in dense random dispersion of cylinders, *J. Comput. Phys.* **136**:629 (1997).
20. Y. Saad and M. H. Schultz, GMRES: a generalized minimum residual algorithm for solving nonsymmetric linear systems, *SIAM J. Sci. Stat. Comput.* **7**:856–869 (1986).
21. Z. Hashin and S. Shtrikman, A variational approach to the theory of effective magnetic permeability of multiphase materials, *J. Appl. Phys.* **33**:3125 (1962).
22. D. A. G. Bruggeman, Berechnung verschiedener physikalischer Konstanten von heterogenen Substanzen, *Ann. Physik* **24**:636 (1935).
23. L. Greengard and V. Rokhlin, A new version of the Fast Multipole Method for the Laplace equation in three dimensions, *Acta Numerica 1997* (Cambridge University Press, Cambridge, 1997), pp. 229–269.

Communicated by J. L. Lebowitz